Yousuke Kakitsubata, MD
Robert D. Boutin, MD
Daphne J. Theodorou, MD
Roger M. Kerr, MD
Lynne S. Steinbach, MD
Karence K. Chan, MD
Mini N. Pathria, MD
Parviz Haghighi, MD
Donald Resnick, MD

Calcium Pyrophosphate Dihydrate Crystal Deposition in and around the Atlantoaxial Joint: Association with Type 2 Odontoid Fractures in Nine Patients[1]

PURPOSE: To investigate the histopathologic anatomy of calcium pyrophosphate dihydrate (CPPD) crystal deposition in and around the atlantoaxial joint and the association between CPPD crystal deposition and subchondral cysts, erosions, and fracture involving the odontoid process of the axis.

MATERIALS AND METHODS: One adult cadaver demonstrating calcification in the retro-odontoid area at computed tomography (CT) was selected for further radiography, CT, and magnetic resonance (MR) imaging at the C1-2 level. Anatomic sectioning and histologic evaluations were performed in the specimen. For clinical study, radiographs ($n = 5$), CT scans ($n = 8$), and MR images ($n = 6$) in nine patients (mean age, 74.4 years) with odontoid process fractures and CPPD crystal deposits in and around the atlantoaxial joint were reviewed.

RESULTS: In the cadaveric specimen, radiography and CT demonstrated calcifications in the transverse ligament; histologic evaluation confirmed that these calcifications were CPPD crystal deposits. In all nine patients, radiography ($n = 5$) and CT ($n = 8$) also showed calcification in areas adjacent to the odontoid process, which included the transverse ligament. T1- and T2-weighted MR imaging showed a retro-odontoid mass of low signal intensity that compressed the cervical cord in six patients. CT, MR imaging, or both demonstrated subchondral cysts, osseous erosions, or a type 2 odontoid fracture in all patients.

CONCLUSION: CPPD crystal deposition disease involving the C1-C2 articulation can be a clinically important entity that may place affected patients at increased risk of pathologic fracture of the odontoid process.

Calcium pyrophosphate dihydrate (CPPD) crystal deposition can be seen in various spinal structures, such as intervertebral disks, ligaments, bursae, articular cartilage, synovium, and joint capsules (1). Although clinically important involvement of spinal ligaments by CPPD crystal deposition is unusual, it rarely causes arthritis-like symptoms or compressive myeloradiculopathy (2–5). CPPD crystal deposition in the transverse ligament of the atlas has been reported in patients with CPPD crystal deposition disease, articular chondrocalci-nosis, or advanced degenerative changes of the atlantoaxial joint (6–8). However, an association between CPPD crystal deposits in and around the atlantoaxial joint and subchondral cysts, osseous erosions, or fracture involving the odontoid process of the axis has not been reported.

The purpose of our study was twofold. Our first objective was to investigate the imaging appearance and histopathologic anatomy of CPPD crystal deposition in the transverse ligament of the atlas in a cadaveric spine. Our second objective was to investigate the association between CPPD crystal deposition and subchondral cysts, osseous erosions, and fractures involving the odontoid process of the axis in nine clinical cases.
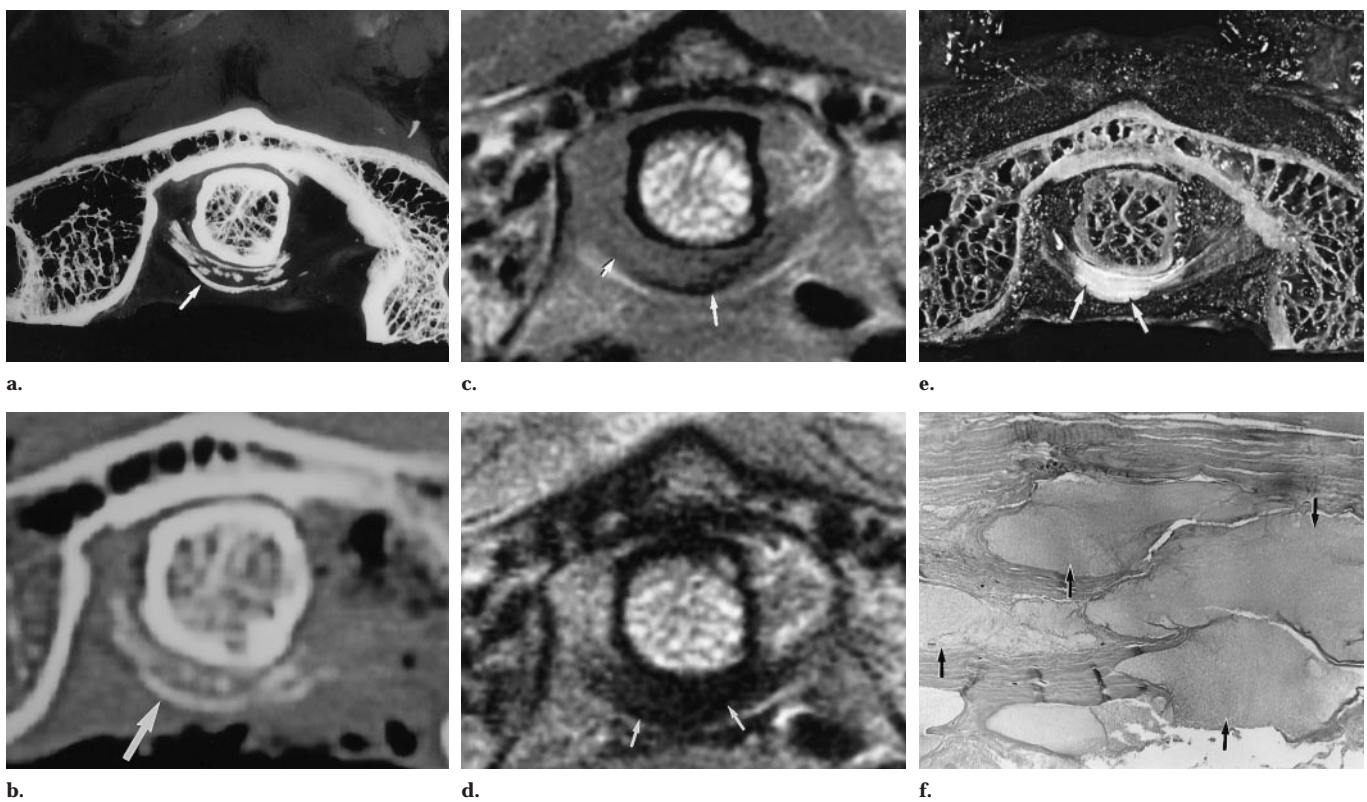
Figure 1. CPPD crystal deposition in the transverse ligament of a cadaveric specimen. **a–c** are of sections at approximately the same level; **d–f** are of a section 4 mm more inferior. **(a)** Radiograph of the pathologic section shows curvilinear and spotty calcifications (arrow) in the transverse ligament. **(b)** Transverse CT scan shows a curvilinear calcification (arrow) in the retro-odontoid region. **(c)** Transverse T1-weighted SE MR image (500/13) shows the transverse ligament with intermediate signal intensity (short arrow). The calcification is shown as a subtle curvilinear low-signal-intensity area (long arrow). **(d)** Transverse T2-weighted SE MR image (4,000/76) shows low-signal-intensity areas (arrows) in the central portion of the transverse ligament. This section is immediately adjacent to those displayed in **a–c** and is at the same level as the section displayed in **e**. **(e)** Photograph of a pathologic specimen shows whitish CPPD crystal deposits (arrows) in the transverse ligament. **(f)** Photomicrograph of specimen depicted in **e** that was obtained from the transverse ligament shows large ''lakes'' of crystal deposition (arrows) within the ligament. (Hematoxylin-eosin stain; original magnification, ×40.)

MATERIALS AND METHODS

Cadaveric Study

One adult cadaver that demonstrated calcification in the retro-odontoid area at computed tomographic (CT) scanning was selected for this study. Subsequently, CT images were obtained from the occipital base through the axis with a section thickness of 2 mm. Magnetic resonance (MR) imaging also was performed at the level of odontoid process by using T1-weighted spin-echo (SE) (repetition time msec/echo time msec [500/13]), fast SE intermediate-weighted (4,000/19), and fast T2-weighted SE (4,000/76) sequences in the transverse plane.

After CT scanning and MR imaging, the cadaveric specimen was sectioned at 2-mm intervals between the occiput and C2. Radiography with high-resolution film (Faxitron; Hewlett-Packard, Palo Alto, Calif) then was performed in these sections.

Histologic sections of C1-C2 were pre-pared with hematoxylin-eosin staining and were then correlated with radiographic, CT, and MR imaging findings by a musculoskeletal radiologist (Y.K.) and an orthopedic pathologist (P.H.).

Clinical Study

Imaging studies from nine patients with odontoid process fractures and CPPD crystal deposits in the transverse ligament of the atlas were collected over 5 years from the teaching files of musculoskeletal radiologists at four institutions. The ages of the patients ranged from 56 to 84 years (mean age, 74.4 years). Seven patients were men and two patients were women. There was a history of motor vehicle accident in two patients, a history of a minor fall (from either a standing position or down one or two steps) in three patients, and no history of trauma in four patients. All nine patients experienced acute onset of neck pain, and three of these patients experienced cervical myelopathy. In patients who experienced trauma, imaging was performed within a week of injury.

Cases were reviewed retrospectively by two musculoskeletal radiologists (Y.K., R.D.B.) who reached agreement by consensus. For each imaging examination, the reviewers recorded the distribution of the calcifications and evaluated osseous erosions, subchondral cysts, joint space narrowing, osteophytosis, sclerosis, odontoid process fracture, retro-odontoid mass, and (on MR images) signal intensity changes in and adjacent to the atlantoaxial joint. CPPD crystal deposition was diagnosed on the basis of its characteristic appearance (7,8) in all nine patients. Surgical and histopathologic confirmation of these imaging findings was available in three patients.

Conventional radiographs (odontoid and lateral views) were available at the time of review in five patients. Radio-

Clinical and Imaging Features in Nine Patients with CPPD Crystal Deposition Disease in and around the Atlantoaxial Joint

Characteristic	Patient 1	2	3	4	5	6	7	8	9
Age (y)	56	70	71	72	75	77	81	84	84
Sex	M	M	F	M	M	M	M	M	F
Trauma history	+	−	−	+	+	+	−	+	−
Myelopathy at clinical examination	+	+	−	−	−	−	−	+	−
Calcification at CT									
Transverse ligament	+	+	+	+	+	+	+	NE	+
Periodontoid	+	−	+	+	+	−	+	NE	+
Synchondrosis	+	−	+	+	−	−	NE	NE	+
Subchondral cyst at CT or MR imaging									
Odontoid process of C2	+	++	+	++	+	+	+	NE	+
Body of C2	++	+	+	++	++	+	+	NE	++
Atlantoaxial joint at CT or MR imaging									
Narrowing	+	+	Fusion	+	−	Fusion	+	NE	−
Osteophytosis	+	−	+	−	−	−	−	NE	−
Sclerosis	+	+	+	+	+	−	−	NE	−
Gas attenuation or signal intensity	−	−	−	+	−	−	−	NE	−
Subluxation	−	−	−	−	−	−	−	NE	+
Odontoid erosion at CT or MR imaging	++	++	++	+	+	+	++	++	++
Odontoid fracture at CT or MR imaging	+	+	+	+	+	+	+	+	+
Retro-odontoid mass at CT or MR imaging	+	+	+	−	−	−	+	+	+
Retro-odontoid mass signal intensity at MR imaging									
T1-weighted image	Low	Low	NE	NE	NE	NE	Low	Low	Low
T2- or T2*-weighted image	Low	Low	Low	NE	NE	NE	Low	High	Low
Gadolinium-enhanced T1-weighted image	NE	NE	NE	NE	NE	NE	Rim	Rim	NE
Cord compression at CT or MR imaging	+	+	+	−	−	−	+	+	+
Edema in cord at MR imaging	−	+	+	NE	NE	NE	+	−	+

Note.—F = female, M = male, NE = not evaluated, Rim = rim enhancement, − = absent, + = present, ++ = markedly present.

graphs of other articulations were not available for review.

CT scanning was performed in eight patients by using a section thickness of 1, 1.5, or 3 mm; two-dimensional reconstructed (coronal and sagittal) images also were available in five patients.

MR imaging was performed in six patients. The imaging algorithms used to evaluate these patients varied because cases were collected from different institutions retrospectively. T1-weighted SE images (500–708/12–15) were obtained in five patients, T2-weighted SE images (2,696/102) were obtained in one patient, T2-weighted fast SE images (3,400–5,000/85–95; echo train length, four to 16) were obtained in four patients, and T2*-weighted gradient-echo images (350–600/15–20; flip angle, 15°–20°) were obtained in two patients. Gadolinium-enhanced T1-weighted SE MR images (500–550/15–21) were obtained in two patients. For each patient examined with MR imaging, both transverse and sagittal images were reviewed.

RESULTS

Cadaveric Study

Radiographs of the pathologic sections clearly demonstrated curvilinear and spotty calcifications in the transverse ligament (Fig 1a).

CT scans of the C1-C2 articulation showed curvilinear calcifications in the retro-odontoid region, which included the anterior and posterior fibers of the transverse ligament (Fig 1b). A small amount of calcification also was present in the anterior and posterior aspects of the atlantoaxial joint. The odontoid process was slightly eroded and displaced to the right side. In the cadaveric specimen, no fracture of the odontoid process was observed.

MR images showed that the transverse ligament was of intermediate signal intensity on both T1-weighted SE images and fast SE intermediate-weighted images and low signal intensity on T2-weighted SE images (Fig 1c, 1d). Portions of the transverse ligament with CPPD crystal deposits demonstrated low signal intensity on T1-weighted SE images; this abnormal appearance was less conspicuous on the MR images than on the CT scans.

Upon gross and histologic inspection of the sectioned specimen, multiple CPPD crystal deposits were observed in the transverse ligament (Fig 1e, 1f). Microscopic inspection with hematoxylin-eosin staining and polarized light did not reveal any other types of crystals.

Clinical Study

Clinical and radiologic features of our nine patients are summarized in the Table.

Conventional radiography (*n* = 5) and transverse CT scanning (*n* = 8) showed calcification behind the odontoid process in all nine patients. With CT scanning, this calcification was curvilinear or stippled in appearance. The distribution of the calcification corresponded to the known anatomic location of the transverse ligament in all cases. In six cases, calcifications also were observed in the periodontoid region: anterior to the transverse ligament, in the remnant of the synchondrosis of C2, or both (Fig 2).

Subchondral cysts or erosions involving the odontoid process were observed to various degrees in all patients. These findings were prominent features in five cases and were most remarkable along the remnant of the synchondrosis of C2. A type 2 odontoid fracture was seen in each of the cases. Two-dimensional reformatted CT images in the coronal or sagittal plane clearly demonstrated the distribution of the calcifications and the odontoid fractures in five cases (Fig 3).

The fracture line was of low signal intensity on either the T1-weighted or the T2-weighted SE MR images. MR images showed the signal intensity changes of marrow edema in the odontoid process, the C2 body, and the anterior arch of C1. Narrowing, gas attenuation or signal
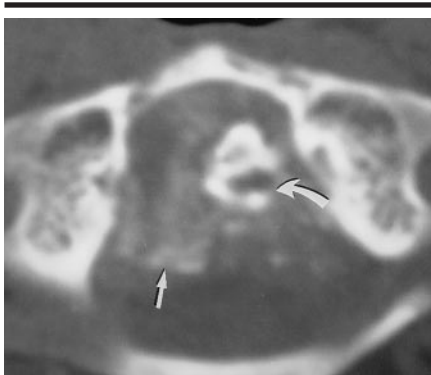
Figure 2. Transverse CT scan obtained in an 84-year-old woman with CPPD crystal deposition disease, atlantoaxial subluxation, and odontoid fracture shows massive calcifications (straight arrow) around the odontoid process of the axis. Atlantoaxial subluxation and erosion of the odontoid process (curved arrow) are seen.

a.

b.

Figure 3. CT scans obtained in a 72-year-old man with type 2 odontoid fracture sustained after a fall down a step. **(a)** Transverse CT scan shows small erosions (straight solid arrows) and a subchondral cyst (curved arrow) in the odontoid process. Calcifications (open arrow) around the odontoid process are observed. The anterior median aspect of the atlantoaxial joint space (arrowheads) is narrowed. **(b)** CT scan reformatted in the sagittal plane shows a type 2 odontoid fracture (long straight arrow) and calcifications (short straight arrows). Gas attenuation (curved arrow) in the anterior aspect of the atlantoaxial joint also is observed.

intensity, osteophytosis, or sclerosis (or various combinations of these findings) involving the anterior median aspect of the atlantoaxial joint also were observed in seven cases, which is consistent with arthropathy owing to CPPD crystal deposition. Anterior atlantoaxial subluxation was observed in one case.

A retro-odontoid mass compressing the cervical cord was observed with CT scanning or MR imaging in six cases. MR imaging also showed the signal intensity changes of marrow edema in the axis and atlas in these cases. The signal intensity of the retro-odontoid mass was relatively low on T1-weighted SE images (compared with the signal intensity of the marrow) in all five cases evaluated with this pulse sequence. On the T2- or T2*-weighted images, the retro-odontoid mass was hypointense to the marrow in five cases (Fig 4) and hyperintense to the marrow in one case. Rim enhancement around the mass was observed in two cases.

In the spinal cord at the level of the retro-odontoid mass, a high-signal-intensity area was observed on T2-weighted MR images in four cases. High signal intensity in the spinal cord on T2-weighted images may be secondary to contusion, myelomalacia, ischemia, or other abnormalities (eg, demyelination, neoplasm). The presence or absence of abnormal signal intensity of the spinal cord in our four cases did not correlate with the clinical manifestations of cervical myelopathy.

Surgery was performed in three patients to stabilize the fractured odontoid process and débride the mass in the peri-
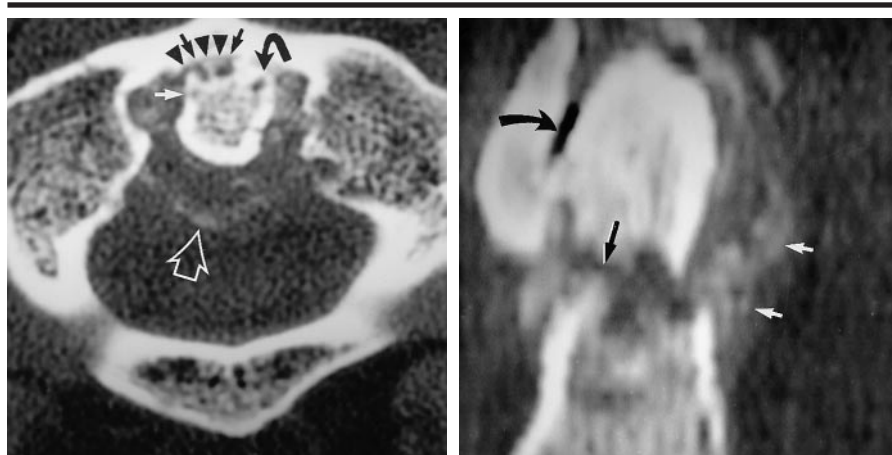
odontoid region. Histologic examination of the surgical specimens showed granulation tissue, fibrous tissue, and cartilaginous tissue. Nodular deposits of birefringent CPPD crystals and crystals of rhomboid shape could be identified with compensated polarized light microscopy and with conventional microscopy, respectively, after staining the sections with hematoxylin-eosin. Hemosiderin deposits in the resected tissues were not observed.

DISCUSSION

The articulation between the atlas and axis comprises three or four synovial joints (9). We use the term "atlantoaxial joint" to refer to both the anterior and posterior median aspects of the atlantoaxial joint, unless otherwise specified.

Distribution and Prevalence of CPPD Crystal Deposition at the C1-C2 Articulation

The deposition of CPPD crystals is known to occur within various soft tissues, which include cartilage, joint capsules, synovium, bursae, tendons, and ligaments (10). One of the ligaments that may be involved by CPPD crystal deposition is the transverse ligament of the atlas, which is a thick, strong band of collagen fibers that arches behind the odontoid process and maintains contact between the odontoid process and the

anterior arch of C1. When disrupted, atlantoaxial subluxation may result (1,11).

The calcification observed in the transverse ligament may be curvilinear, stippled, or mixed. Although the mixed appearance was common in our cases, curvilinear calcifications in the retro-odontoid region are strongly suggestive of CPPD crystal deposition in the transverse ligament of the atlas (7,8). In our cadaveric study, we confirmed that the characteristic appearance and location of calcifications were indeed secondary to CPPD crystal deposition.

Deposits of CPPD crystals in the transverse ligament are not rare and are most likely associated with aging, degenerative disease, or a disorder in metabolism. The prevalence of calcific deposits within the transverse ligament varies according to the patient population that is studied (6–8) from 5.7% in unselective patients undergoing CT scanning of the brain or paranasal sinuses (7) to 66% in patients with articular chondrocalcinosis (8).

Complications of CPPD Crystal Deposition at the C1-C2 Articulation

In patients with CPPD crystal deposition disease, numerous vertebral abnormalities have been reported, including degenerative disk disease, vertebral destruction, scoliosis, spondylolisthesis, atlantoaxial subluxation, vertebral ankylosis, occipitoatlantoaxial joint collapse, and thickening of spinal ligaments (1,11–
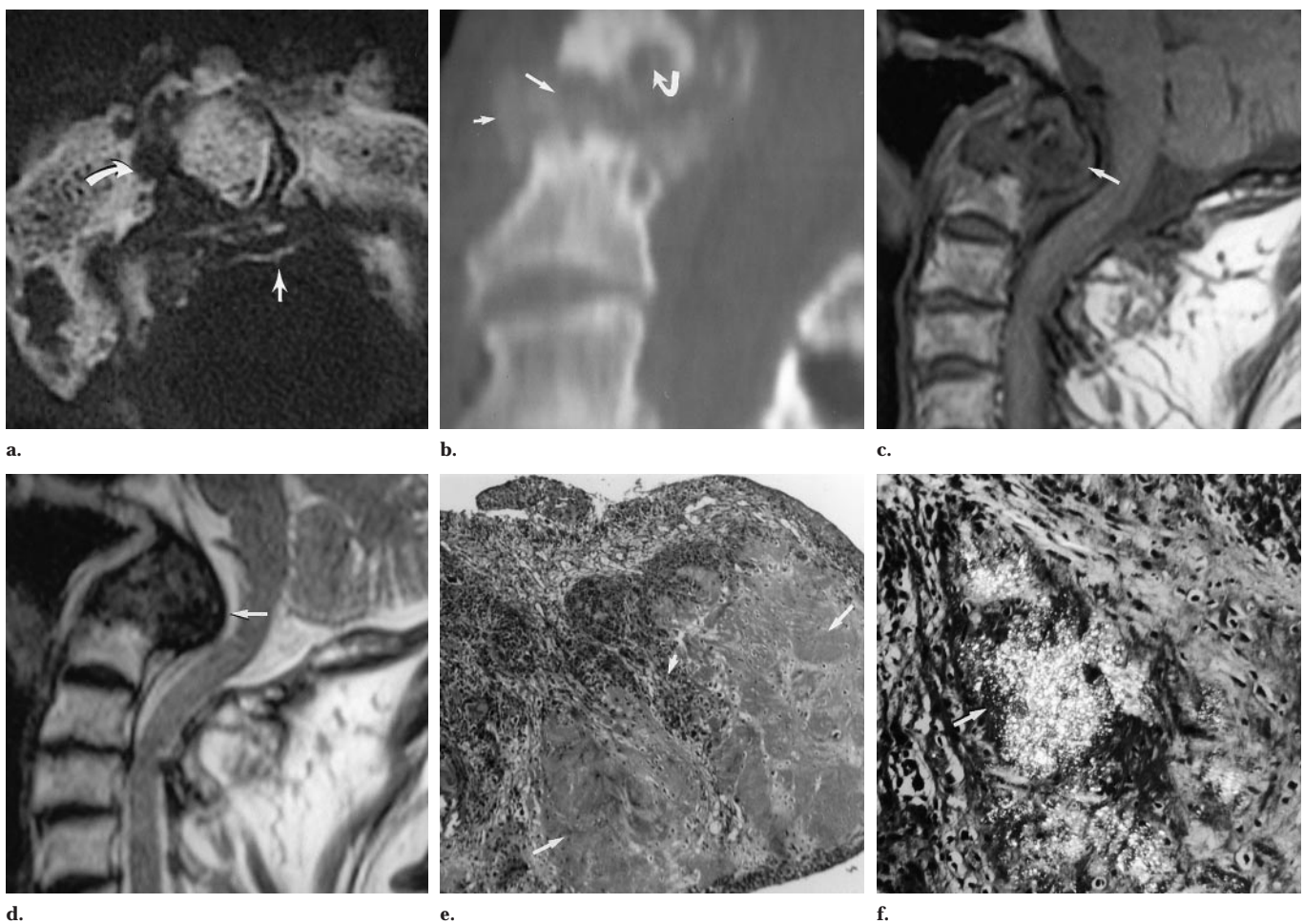
Figure 4. Images obtained in a 56-year-old man with CPPD crystal deposition disease, traumatic type 2 odontoid fracture, and retro-odontoid mass. **(a)** Transverse CT scan shows calcifications (straight arrow) around the odontoid process. Atlantoaxial joint space narrowing and destructive changes involving the atlas (curved arrow) are observed. **(b)** CT scan reformatted in the sagittal plane demonstrates periodontoid calcification (short straight arrow), cystic changes in the dens (curved arrow), and a type 2 odontoid fracture (long straight arrow). **(c)** Sagittal T1-weighted SE MR image (705/15) shows a retro-odontoid mass (arrow) compressing the cervical spinal cord. The signal intensity of the retro-odontoid mass is low compared with that of the spinal cord and bone marrow. **(d)** On the T2-weighted fast SE MR image (4,282/94), the signal intensity of the retro-odontoid mass (arrow) is low compared with that of the spinal cord and bone marrow. **(e)** Photomicrograph shows a large crystal deposit (long arrows) as pale nodules with hyalinization bordered by inflammatory cells (short arrow). (Hematoxylin-eosin stain; original magnification, ×16.) **(f)** Photomicrograph obtained by using a polarizing lens demonstrates crystal deposits (arrow) in the lesion. (Hematoxylin-eosin stain; original magnification, ×40.)

14). Destructive and hypertrophic arthropathy of the cervical spine with associated ossific fragmentation also has been reported (15). In our study, CT scanning showed osseous abnormalities of the odontoid process, such as subchondral cysts or erosions, in all cases. Among the bone changes, subchondral cyst formation was especially prominent. This feature is interesting, because conspicuous subchondral cyst formation in the peripheral joints is typical of CPPD crystal deposition even when calcification is not present (10).

Massive CPPD crystal deposits with bone erosion involving the cervical vertebrae have been reported previously (16–18). In our six cases with a soft-tissue mass, the odontoid process also was markedly eroded. In these cases, a retro-odontoid mass containing CPPD crystals may have resulted in erosion or destruction of the odontoid process. Bone erosion has not been reported as a dominant feature of CPPD crystal deposition disease in the peripheral joints and is generally considered a finding that suggests an alternative diagnosis (eg, rheumatoid arthritis) (14,19). Our study findings, however, suggest that CPPD crystal deposition in the transverse ligament can be associated with erosion of the odontoid process.

To our knowledge, a relationship between the CPPD deposition in and around the C1-C2 articulation and odontoid fracture has not been reported previously. Radiographs of other articulations were not available for review, which would have allowed assessment of whether the CPPD crystal deposition was primary rather than secondary in relation to the odontoid fracture. In our series of patients, a type 2 odontoid fracture was seen in patients with histories of major trauma ($n = 2$), minor trauma ($n = 3$), or no trauma at all ($n = 4$). We recognize that CPPD crystal deposition may occur as a complication of trauma (20) but believe that CPPD crystal deposition secondary to injury is unlikely because CPPD crystals were evident within 1 week of the traumatic episode in our patients. Although the exact relationship of the odon-

toid fractures and the CPPD crystal deposits about the odontoid process is unclear, we have found that massive CPPD crystal deposition in the periodontoid soft tissues may be associated with erosions and subcortical cysts at the base of the odontoid process. Our results suggest that these structural changes may weaken the odontoid process and predispose it to subsequent fracture.

Imaging of CPPD Crystal Deposition at the C1-C2 Articulation

Radiography readily demonstrated CPPD crystal deposits adjacent to C1-2 in our sectioned specimen. However, in our clinical patients, periodontoid CPPD crystal deposition was either subtle or undetectable with routine radiography because of superimposition of adjacent osseous structures.

CT scanning generally is regarded as sensitive for the detection of small calcifications. In our cases, this technique was useful for the detection of CPPD crystal deposition adjacent to the odontoid process, which included deposits in the transverse ligament. These CPPD crystal deposits adjacent to C1 and C2 presumably were the cause of pyrophosphate arthropathy of the anterior median aspect of the atlantoaxial joint.

MR imaging can demonstrate the normal or abnormal transverse ligament to good advantage (21–24). Although MR imaging has a lower sensitivity for the detection of calcification than CT scanning, it can display massive CPPD crystal deposition in the transverse ligament and atlantoaxial joint (17,18,25–27). Indeed, assessment of the extent of the cartilage and bone destruction by CPPD crystal deposition also is considered an indication for MR imaging (20,25,28,29). Moreover, MR imaging can show ligamentous abnormalities, such as rupture and osteoperiosteal avulsion (21), and the relatively low signal intensity of the retro-odontoid mass on T2-weighted MR images may be helpful in differentiating massive CPPD crystal deposition from most neoplasms. MR imaging also shows the condition (eg, degree of compression, abnormal signal intensity) of the neighboring spinal cord to best advantage.

Zünkeler et al (27) have reported that massive CPPD crystal deposition is visualized as a mostly isointense mass on T1-weighted MR images, a mass of varying signal intensity (ranging from hypo- to hyperintense) on T2-weighted images, and a peripherally enhancing mass on gadolinium-enhanced images. In cases of massive CPPD crystal deposition in the ligamentum flavum, both T1- and T2-weighted MR images reveal hypointense foci (29–31). Some rare cases of CPPD crystal deposition disease may manifest as increased signal intensity on T1-weighted SE images (32), although this was not observed in our series.

In our cases, MR images clearly showed a retro-odontoid mass, and its signal intensity was relatively low compared with that of marrow on T1- and T2-weighted images in five cases and high on T2*-weighted images in one case. Rim enhancement around the mass was observed in both cases in which gadolinium-based contrast material was administered. The signal intensity of the massive crystal deposits may vary with the composition and concentration of the calcium crystals, the inconstant presence of associated granulation tissue and fibrosis, or other factors. No hemosiderin deposits were observed with histologic analysis in our cases.

Our study has two major limitations. First, the number of cases that we evaluated was limited, so defining the relationship among CPPD crystal deposition, pyrophosphate arthropathy of the atlantoaxial joint, and pathologic odontoid fractures will require a larger study. We suspect that such fractures are relatively rare but believe this entity merits reporting in an initial series. Second, our study was retrospective, without control subjects, and without histologic proof in all cases. We chose to report our experience at this time in hopes of prompting recognition—and further study—of this potentially debilitating injury in patients with CPPD crystal deposition disease. Given that we studied images only in patients with both CPPD crystal deposition and fractures, this study has a substantial selection bias. We do not know the prevalence of odontoid process fractures in patients with spinal CPPD crystal deposition disease. We do believe, however, that the relationship between CPPD crystal deposition disease and odontoid process fractures is more than coincidental.

Our results indicate that CPPD crystal deposition disease in and around the atlantoaxial joint may play a role in placing patients at increased risk of pathologic fracture of the odontoid process. In our cadaveric specimen and patients, CT scanning provided the most conspicuous display of CPPD crystal deposition in the periodontoid soft tissues, pyrophosphate arthropathy of the atlantoaxial joint, and erosions and cysts in the odontoid process that presumably placed our patients at increased risk for fracture of the dens. Although the CPPD crystal deposits generally were not as conspicuous with MR imaging as with CT scanning, MR imaging demonstrated to best advantage the presence of CPPD crystal–associated retro-odontoid masses and associated spinal cord impingement. Both CT scanning and MR imaging effectively demonstrated the pathologic fractures at the base of the odontoid process in these patients with CPPD crystal deposition disease.

References
1. Resnick D, Pineda C. Vertebral involvement in calcium pyrophosphate dihydrate crystal deposition disease: radiographic-pathological correlation. Radiology 1984; 153:55–60.
2. Burguet JL, Sick H, Dirheimer Y, Wackenheim A. CT of the main ligaments of the cervico-occipital hinge. Neuroradiology 1985; 27:112–118.
3. Gomez H, Chou SM. Myeloradiculopathy secondary to pseudogout in the cervical ligamentum flavum: case report. Neurosurgery 1989; 25:298–302.
4. Baba H, Maezawa Y, Kawahara N, Omita K, Furusawa N, Imura S. Calcium crystal deposition in the ligamentum flavum of the cervical spine. Spine 1993; 18:2174–2181.
5. Kawano N, Yoshida S, Ohwada T, Yada K, Sasaki K, Matsuno T. Cervical radiculomyelopathy caused by deposition of calcium pyrophosphate dihydrate crystals in the ligamenta flava: case report. J Neurosurg 1980; 52:279–283.
6. Dirheimer Y, Bensimon C, Christmann D, Wackenheim C. Syndesmo-odontoid joint and calcium pyrophosphate dihydrate deposition disease (CPPD). Neuroradiology 1983; 25:319–321.
7. Zapletal J, Hekster REM, Straver JS, Wilmink JT, Hermans J. Association of transverse ligament calcification with anterior atlanto-odontoid osteoarthritis: CT findings. Neuroradiology 1995; 37:667–669.
8. Constantin A, Marin F, Bon E, Fedele M, Lagarrigue B, Bouteiller G. Calcification of the transverse ligament of the atlas in chondrocalcinosis: computed tomography study. Ann Rheum Dis 1996; 55:137–139.
9. Williams PL, Warwick R. Arthrology. In: Williams PL, Warwick R, eds. Anatomy of the human body. 36th ed. Philadelphia, Pa: Saunders, 1980; 419–503.
10. Uri DS, Dalinka MK. Crystal disease. Radiol Clin North Am 1996; 34:359–374.
11. Salcman M, Khan A, Symonds DA. Calcium pyrophosphate arthropathy of the spine: case report and review of the literature. Neurosurgery 1994; 34:915–918.
12. Markiewitz AD, Boumphrey FR, Bauer TW, Bell GR. Calcium pyrophosphate dihydrate crystal deposition disease as a cause of lumbar canal stenosis. Spine 1996; 21:506–511.

13. Ojemann JG, Grubb RL, Kyriakos M, Baker KB. Calcium carbonate apatite deposition in the cervical spine with associated vertebral destruction: case report. J Neurosurg 1997; 86:1022–1026.
14. Resnick D, Niwayama G, Goergen TG, et al. Clinical, radiographic and pathologic abnormalities in calcium pyrophosphate dihydrate deposition disease (CPPD): pseudogout. Radiology 1977; 122:1–15.
15. Gerster JC, Doenz F. Unusual destructive and hypertrophic arthropathy of the atlanto-axial joint in calcium pyrophosphate dihydrate deposition disease. Osteoarthritis Cartilage 1994; 2:275–279.
16. Ciricillo SF, Weinstein PR. Foramen magnum syndrome from pseudogout of the atlanto-occipital ligament: case report. J Neurosurg 1989; 71:141–143.
17. Wells CR, Morgello S, DiCarlo E. Cervical myelopathy due to calcium pyrophosphate dihydrate deposition disease (letter). J Neurol Neurosurg Psychiatry 1991; 54:658–659.
18. Fidler WK, Dewar C, Fenton PV. Cervical spine pseudogout with myelopathy and Charcot joints. J Rheumatol 1996; 23:1445–1448.
19. Resnick D, Williams G, Weisman MH, Slaughter L. Rheumatoid arthritis and pseudo-rheumatoid arthritis in calcium pyrophosphate dihydrate crystal deposition disease. Radiology 1981; 140:615–621.
20. Ishida T, Dorfman H, Bullough PG. Tophaceous pseudogout (tumoral calcium pyrophosphate dihydrate crystal deposition disease). Hum Pathol 1995; 26:587–593.
21. Dickman CA, Mamourian A, Sonntag VK, Drayer BP. Magnetic resonance imaging of the transverse atlantal ligament for the evaluation of atlantoaxial instability. J Neurosurg 1991; 75:221–227.
22. Greene KA, Dickman CA, Marciano FF, Drabier J, Drayer BP, Sonntag VK. Transverse atlantal ligament disruption associated with odontoid fractures. Spine 1994; 19:2307–2314.
23. Yu S, Haughton VM, Rosenbaum AE. Magnetic resonance imaging and anatomy of the spine. Radiol Clin North Am 1991; 29:691–710.
24. Schweitzer ME, Hodler J, Cervilla V, Resnick D. Craniovertebral junction: normal anatomy with MR correlation. AJR Am J Roentgenol 1992; 158:1087–1090.
25. El-Khoury GY, Tozzi JE, Clark CR, Foucar E, Menezes AH, Smoker WR. Massive calcium pyrophosphate crystal deposition at the craniovertebral junction. AJR Am J Roentgenol 1985; 145:777–778.
26. Rivera-Sanfeliz G, Resnick D, Haghighi P, Wong W, Lanier T. Tophaceous pseudogout. Skeletal Radiol 1996; 25:699–701.
27. Zünkeler B, Schelper R, Menezes AH. Periodontoid calcium pyrophosphate dihydrate deposition disease: "pseudogout" mass lesions of the craniocervical junction. J Neurosurg 1996; 85:803–809.
28. Resnick D, Niwayama G. Calcium pyrophosphate dihydrate (CPPD) deposition disease. In: Resnick D, ed. Diagnosis of bone and joint disorders. 3rd ed. Philadelphia, Pa: Saunders, 1995; 1556–1610.
29. Shaffrey CI, Munoz EL, Sutton CL, Alston SR, Shaffrey ME, Laws ER Jr. Tumoral calcium pyrophosphate dihydrate deposition disease mimicking a cervical spine neoplasm: case report. Neurosurgery 1995; 37:335–339.
30. Sato R, Takahashi M, Yamashita Y, et al. Calcium crystal deposition in cervical ligamentum flavum: CT and MR findings. J Comput Assist Tomogr 1992; 16:352–355.
31. Brown TR, Quinn SF, D'Agostino AN. Deposition of calcium pyrophosphate dihydrate crystals in the ligamentum flavum: evaluation with MR imaging and CT. Radiology 1991; 178:871–873.
32. Burke BJ, Escobedo EM, Wilson AJ, Hunter JC. Chondrocalcinosis mimicking a meniscal tear on MR imaging. AJR Am J Roentgenol 1998; 170:69–70.